ingegneria sismica
International Journal of Earthquake Engineering
Anno XLIII - Num. 2 - 2026

Influence of Atmospheric Intraseasonal Oscillations on Land Surface Temperature in Shanxi

Jinxia Wang[1,*], *Yan Wang*[1] *and Ziyu Yan*[1]

[1] Yangquan Meteorological Bureau of Shanxi Province, Yangquan 045000, Shanxi, China

SUMMARY: *To determine the impact of daily reanalyses data and real-time multivariate Madden-Julian Oscillation (RMM) indices from 1985 to 2025 on surface temperatures across Shanxi Province using these datasets. Analysis of the phase-based composite, seasonal stratification, anomaly diagnosis, and 500 hPa teleconnection. The investigation reveals that there are annual variations and phase changes in MJO's influence upon Temperature Distributions of Shanxi Region. During winter, the greatest adjustment occurs; phases 3 to 4 have a province-wide cold anomaly of around −0.8 K, and phases 6 to 8 show warming but their high-point temperature is at about 0.6 K. Spring has lower responsiveness; there are primarily warm anomalies during periods 2-3, and cold ones occur between periods 4-6. Because the MJO signal is dominated by the East Asian summer monsoon background and local convective processes during the summer season, there is relatively weak coherence modulated. In autumn, the response to temperature changes increases again; The cold anomaly at this time is about -0.7K, and the local warm anomaly has reached up to 1.0K, which exceeds the winter warm peak. Physically, MJO-related tropical convection activity can cause Shanxi to be affected through the propagation of extratropical Rossby waves and their associated Eurasia-Pacifi-canteleconnections. Positive 500-hPa geopotential height anomalies over northern China favor warm advection and suppressed cold-air activity, while negative height anomalies favor trough control and cold advection. These results show that the MJO cycle can be used as a good sub-Seasonal predictor of cold-warm phenomena in Shanxi Province during this period every year.*

KEYWORDS: *Madden–Julian oscillation, Shanxi Province, surface temperature, phase composite, teleconnection, extended-range forecasting.*

1 Introduction

Located in East Shaanxi on the eastern edge of the Loess Plateau, stretching across a pronounced elevation drop from the northern plateaus to the central sedimentary basin system and finally entering the South-facing Mountain-Basin transitional zone. Its surface-temperature variability affects winter heating demand, frost-risk management, spring sowing, orchard protection, coal-related energy dispatch and public-weather services. Also situated within both the East Asian monsoon region and the middle-to-high latitude Westerlies belt. The selected locations can respond sensitively to local terrain and remote circulation phenomena simultaneously. In terms of operation prediction, one challenge is that its difficulty level at the short-term sub-seasonal stage exceeds long-range synoptical forecast and falls within short-period seasonal forecasts; Among the above-suggested Signals, there is one whose expected

*wangjinxia.chn@foxmail.com
https://doi.org/10.65102/is2026781
Published: 30 April, 2026

trend persists for more than two weeks; it has been confirmed through regional temperature variation analysis to have a real-world explanation.

The Madden - Julian Oscillation (MJO) is one mode of variation at the midlatitude tropospheric level with significant intraseasonal amplitude on a large domain and long cycle; it consists of three scales: source-scale, propagation-scale and end-location Scale. Despite the origin of the MJO being close to the equator, it causes a diabatic heating anomaly with long-range effects of Rossby waves. In boreal Winter, the active convection associated with tropical Heating may change the North Pacific Wave Group or modify the Eurasian circulation System and East Asian low pressure Activity [1-3]. These circulation changes may be a potential reason for the modulating effect of an equatorial convection anomaly on temperature in northern China.

Based on the continuous enhancement of fundamental methodologies, combined with real-time multivariate MJO indices, using OLRS polar imager data along with Z-layer averaged-wind-fields to track eastern propagating phenomena across all four quadrants of our atmosphere throughout the year is feasible. In terms of the Asia summer monsoon area, after refinement by the boreal summer inter-seasonal oscillation index for the intraseasonal period, northward and northeast-moving propagation convection can be monitored [4, 5]. These indices offer the required Phase Information for linking tropical convection with mid-latitude Surface Responses. In terms of the impact level, winter-time MJO activity has an influence on East Asia's surface-air temperature and cold fronts via large-scale circulation anomaly mechanisms [6]. But because evidence from East Asia or the general Monsoon Zone cannot apply universally to Shanxi Province. The province lies on both sides of two mountains and, as it is close to major cold air intake corridors because of its altitude. These geographical conditions can increase, slow down or diminish the local temperature reaction at the same MJO stage. Therefore, at the province-level composite analysis of this problem, determine which MJO stage corresponds to significant differences in Surface temperature changes over Shanxi and their associated Circulation Types.

The regional problem is therefore specific. Shanxi is not a pure monsoon-controlled area and does not suffer from the impact of west-west Pacific convection directly. Its Winter and Transition Season Temperature is regulated by interactions among Siberian Cold-Air Outbreaks, Eastern Asia Trough Variability, Western Pacific Subtropical Circulation, Local Elevation and Basin Inversion. Only the MJO signal can influence this interaction via intermediary circulation Structures. If the analysis ends up stating a specific MJO phase as warm or cold without supporting data for extended range prediction of temperatures. The phase response relation should be associated with OLGR anomalies, 500-hpa height anomaly fields and seasonal-mean flow patterns.

This paper has found a region's deficiency by using daily data from 1985 to 2025 and dividing the analysis into four periods: winter, spring, summer and autumn. Three related questions are put forward as follows: What is the seasonal evolution of MJO convection in the OLR map? Which MJO phases cause warm and cold surface-temperature anomalies in Shanxi; And how do these phase-specific temperature responses manifest through mid-tropospheric teleconnections? Anomaly detection of RMM phases, Daily anomalous data Construction and Phase Composite Diagnosis. This Design keeps the eight-phase Structure of the original MJO and can evaluate separately the responses in Shanxi across the four seasons.

The contribution of this work is threefold. First, it provides a season-by-season diagnosis of MJO convective evolution and surface-temperature response over a mid-latitude province with complex terrain. Second, it links the temperature response to 500-hPa height anomalies rather than treating the phase composite as a statistical result alone. The third is to determine that the seasons when MJO phase information can more clearly explain cold and warm anomaly changes across China are Winter and Autumn.

The other reasons for an abnormal trend in the prediction of temperatures in Shanxi province are that, together with distant atmospheric circulation systems and regional geographical influences, this kind of anomaly appears. The same synoptic trough may have various thermal Effects on the northwestern plateau area, central Basin and southeastern Valley respectively. Such a Spatial Complexity necessitates use of multiple countries' MJO diagnosis methods. A province-level composite will keep the main circulation signals and determine whether an abnormal area appears reasonable as a result of combining them.

In this study, surface temperature refers to the value of grid-averaged near-surface land thermal fields represented by T2M. This choice keeps the analysis consistent over the full 1985-2025 record and allows surface-temperature response to be linked directly with 500-hPa circulation. Therefore, the interpretation highlights regional thermal anomaly and cold-warm advection instead of satellite skin temperature measurement. The latter does not require that much detail, hence its broader scope in this paper's selected routes.

2 Methods

2.1 Data sources, study period and regional domain

From 1st December 1985 to the end of November in 2025. Following the common definition of seasons based on meteorology: Winter ranges from December to February each year; Spring is from March to May; Summer lasts from June to August; And Autumn spans September to November. Approximately between 34° and 40° north latitude, and between 110° and 115° east longitude. The surrounding area remains in map-composite forms to determine if the Shanxi signal belongs to an extensive north-central region anomaly or a localised reaction.

Using the real-time multivariate MJO index of Wheeler and Hendon [7] to describe MJO activity. Contains the daily RMJL1, RMJL2, MJO phase and MJO strength. RMM1 and RMM2 are obtained by combining the empirical orthogonal function representation of equatorially averaged outgoing long-wave radiation, 850 hPa zonal winds and 200 hPa zonal Winds. Phase space coordinates represent the longitude of the primary tropical convective anomaly; The size is proportional to its intensity level. By convention, the days for which RMM's Amplitude reaches or exceeds 1.0 is considered an Active MJO day. These are the motions of areas that have been affected by this convection throughout various locations on Earth and have subsequently flowed towards central Hawaiian waters.

Tropical convective cloud type determination using the outgoing long-wave radiation method. Negatively correlated with the absence of clouds, positively correlated with clouds; weakly associated with surface conditions. Therefore, as the main variable to confirm that the RMM-phase composite retains expected eastward convective development during a lightning strike. The surface temperature is denoted as T2M in NCEP/NCAR Reanalysis I; The diagnosis of the middle troposphere circulation path for the Shanxi reaction based on 500 hPa geopotential heights will be presented. While T2M differs from satellite-derived skin temperatures, it offers a constant daily land surface thermal diagnosis appropriate for analysis of the last four decades.

Analyse separately the four data components and then compose them together. Only RMM is employed for event identification; OLR can determine whether there are tropical convection areas in this region; T2M acts as the dependent variable in Shanxi Province; And 500 hPa height also has a certain influence on it. To prevent a cyclic interpretation. For instance, a warm anomaly in Shanxi will be attributed to the MJO only if there is a physiologically sound OLR pattern at this time and a mid-tropospheric height anomaly that corresponds to a warm-advective environment.

The length of the study is sufficient to weaken the impact of a few exceptional occurrences; however, the distribution of Phase-S season is still unbalanced due to an imbalanced number of Active-MJO days in different periods. Therefore, in this study, strong and spatially continuous composites are considered more important than isolated grid-point signals. Also listed are priorities in this analysis on phase pairs and Seasonal sequences; there is generally no significant immediate reaction to physical changes in the MJO (isolated disturbances).

Table 1. The data components and analysis functions of the MJO-Shanxi Temperature Composite.

Data component	Variable used in this study	Resolution or temporal form	Role in the analysis
RMM index	RMM1, RMM2, phase, amplitude	Daily	Defines active MJO events and eight-phase classification
NOAA OLR	Outgoing longwave radiation anomaly	Daily gridded field	Diagnoses tropical convection and phase propagation
NCEP/NCAR Reanalysis	T2M and 500-hPa geopotential height	Daily gridded fields	Evaluates Shanxi temperature response and circulation bridge
Regional mask	Shanxi and surrounding northern-China domain	Province-scale target area	Separates the target response from broader circulation background

2.2 MJO event definition and anomaly construction

Construct an event sample at a daily frequency level. Determine the values of RMM-amplitude for every day using their corresponding primary Components. If the amplitude exceeds 1.0, keep that day as a member of one of the eight MJO categories. Days with an amplitude less than 1.0 are not included in the phases to avoid physical meaninglessness of the phase angle under a weak MJO signal. Screening removes weak tropical convective systems to avoid interference with the identification of strong, stable intraseasonal variability.

Daily anomaly calculations for OLR, T2M, and 500-hPa height based on the multi-year daily climatology. Computationally, for each calendar day at all grids' locations, compute the climate data independently. In fact, it might be discarded or treated consistently to maintain the continuity of the general climate pattern. An abnormality Definition used in this study can be described as follows:

$$X'(d,\lambda,\phi) = X(d,\lambda,\phi) - \overline{X}_{c(d)}(\lambda,\phi) \quad (1)$$

In Eq. (1), X represents OLR, T2M or 500-hPa geopotential height; d refers to the target day; λ and φ stand for longitude and latitude; $c(d)$ is a calendar day corresponding to d; and an over-bar indicates the 1985-2025 daily climatology. Anomalies field X' is constructed through this process, removing the seasonal mean component; it then combines daily data across years in each month of a given MJO state.X'

2.3 Composite design and teleconnection interpretation

Composite analysis is conducted independently for each season and the MJO state. For each season s and phase p, collect all active MJO days that meet the RMM-amplitude threshold. The anomaly fields on these days are then averaged to get the phase composite. This Design

maintains the typical canonical MJO phases, but allows for Seasonal variations in convective intensity, extratropical propagation and the response of Shanxi temperature separately. As shown below, the composition of estimators:

$$\overline{X}'_{s,p}(\lambda,\phi) = \frac{1}{N_{s,p}} \sum_{d \in \Omega_{s,p}} X'(d,\lambda,\phi) \tag{2}$$

In Eq. (2), s is the season, A p is the MJO phase, $\Omega_{s,p}$ is the set of active MJO days belonging to season s and phase p, $N_{s,p}$ is the sample size, and the composite field $\overline{X}'_{s,p}$ represents the mean anomaly associated with that phase-season combination. The same estimator is used for OLR, T2M, and 500-hPa height; therefore, the convective sources, regional thermal responses, and circulation bridges can be diagnosed in the same observational data set simultaneously.

Teleconnection Analysis focuses on the spatial relationship among tropical OLR anomalies, 500 hPa Height Anomalies over Eurasia and East Asia. Following explanations in other parts of the paper; the tropical MJO-related heating drives Rossby Waves that affect mid-latitude circulation [8, 9]. The positive 500 hPa height anomaly in the region of Shanxi was interpreted as a favourable circadian condition for warm advection, reduced cold air intrusions, and weak troughs. Negative-height anomaly areas indicate conditions favourable to the intrusion of low temperatures, strong trough control and strengthened cold-air impact. It is not required that at any stage, temperature changes are visibly affected on a surface basis; only to determine if they have some logical relationship with OLR-height relationships.

Composite Techniques rely on observation and thus cannot present things as they really are. A phase is considered significant only if the sign of the Shanxi temperature anomaly, the seasonal OLR pattern and the inferences from 500 hPa circulation states are interpreted as a continuous process. The exclusion of Summer periods based on a smaller range of Temperature deviations, along with dividing Transition season weak anomalies from strong winter and Autumn responses.

3 Results and Discussion

3.1 Seasonal evolution of MJO convection in the OLR composites

First, check if there has been a loss of canonical eastward MJO propagation in the phase samples; Then, if we ascribe this temperature variation to the MJO or some external cause unrelated to it would be difficult. RMM phase space diagram is used to provide a reference for events; As shown in Figure 1.

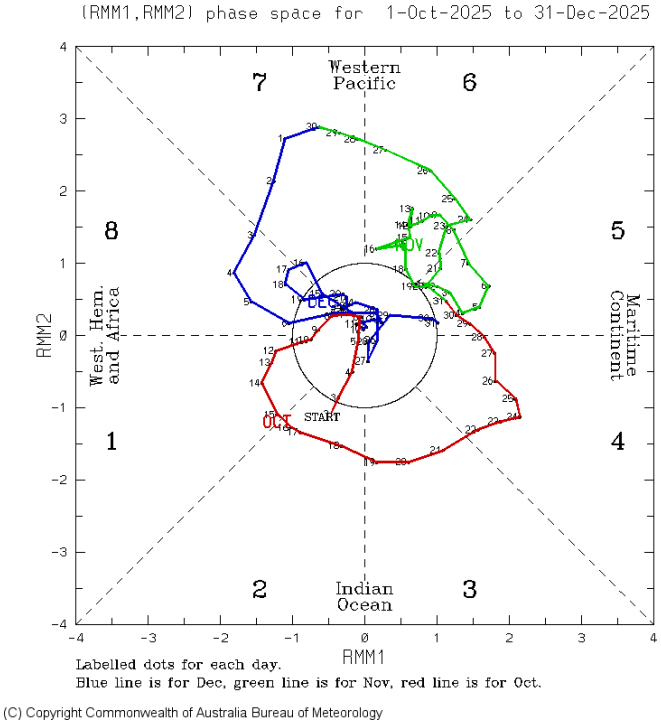

Figure 1: RMM phase-space diagram of the five-phase system from September to November 2025.

Figure 1 is a clockwise phase-space trajectory of RMM1 and RMM2. Each day's point represents a stage of the tropical convective anomaly; The distance from the origin gives an indication of the MJO amplitude. The reference in this stage is only for classifying the active MJO event; Afterwards, it will examine associated OLR, T2M and 500-hPa height anomalies.

OLR composite materials will be tested against the seasonality difference of MJO convection. Winter convection is the strongest and most spatially extensive, as shown in Figure 2.

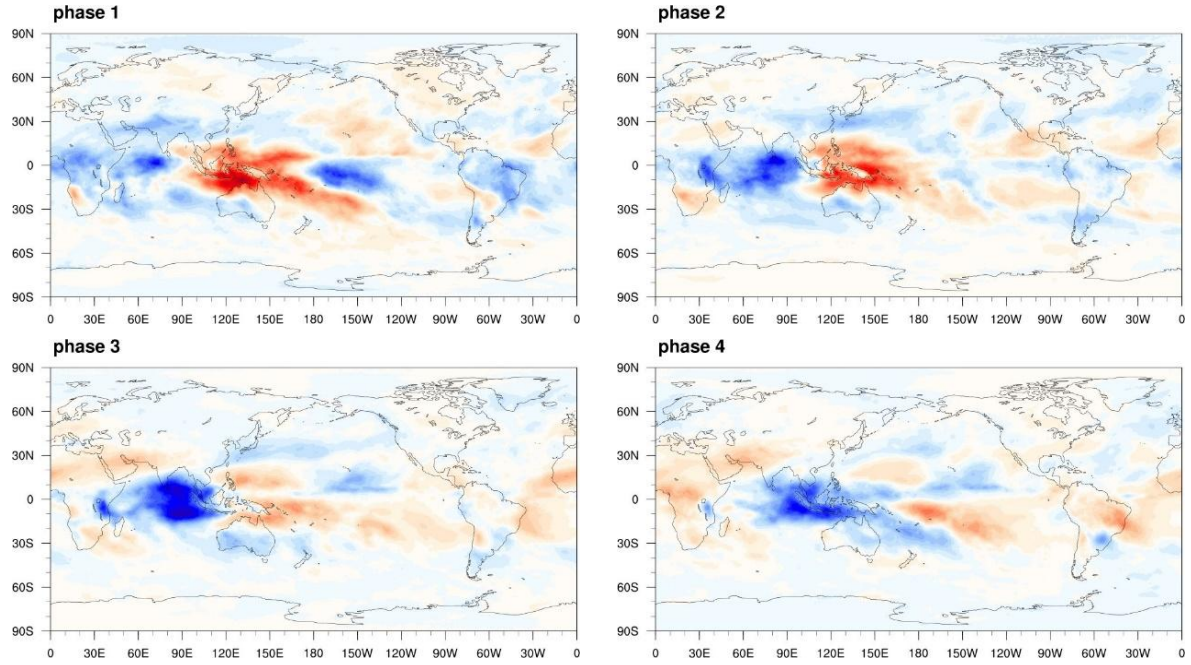

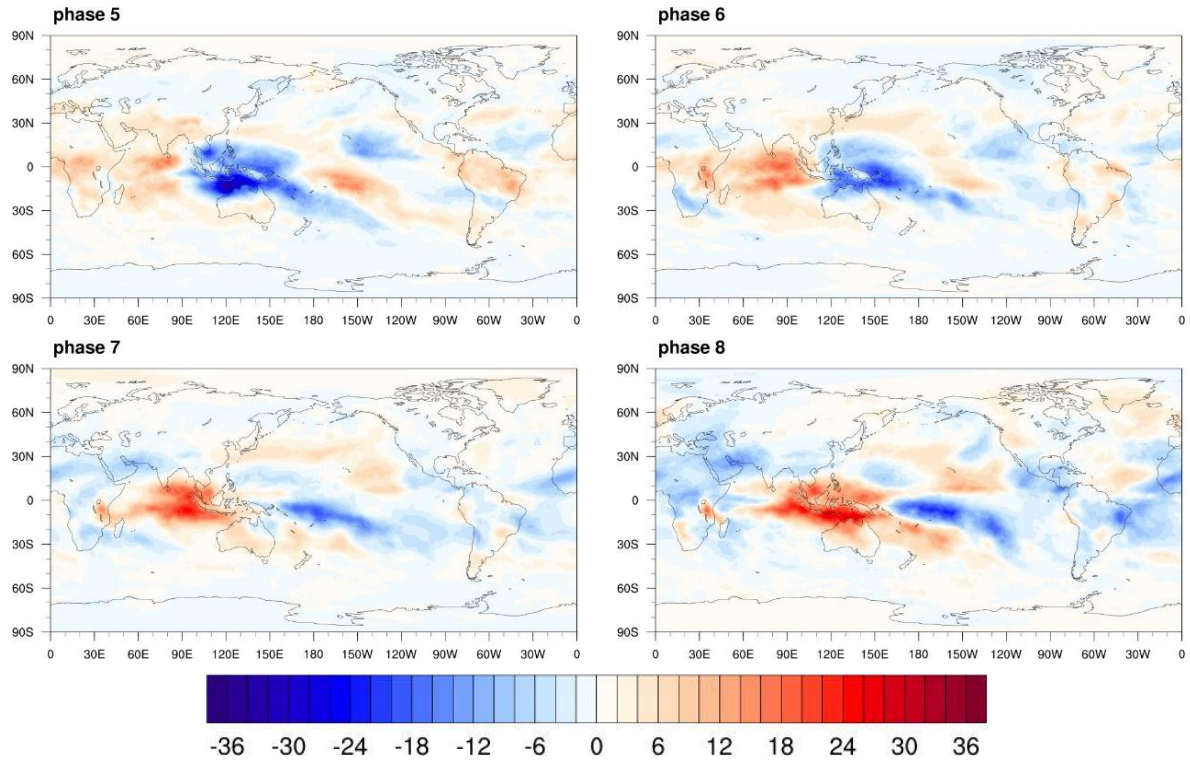

Figure 2: Winter composite OLR anomalies by MJO phase groups (units in W·m^{-2}).

Figure 2 shows that the winter OLR anomaly field follows a clear eastward sequence. During phase 1-2, there is a relatively weak negative OLR anomaly in the western and central part of the Indian Ocean area, while it becomes stronger still-moving-Eastwards. In Phases III-IV, The centre of the negative anomaly is located on the maritime continent, spreading latitudinally; Some areas have extended even to the tropical zone. Phase five-six enhancement of convective activities in the western Pacific region and suppression-convection signals have recovered over phase six. During phases seven-Eight, The negative Centre weakened and migrated to the Central Pacific area. Amplitude is greater than -30 W·m^-2 in the most intense states; In all four seasons, only the winter composite exhibits a wide-ranging tropic-extreme condition region.

The spring OLR composite retains the same phase progression, but the convective anomaly is weaker and less connected to the extratropical belt, as shown in Figure 3.

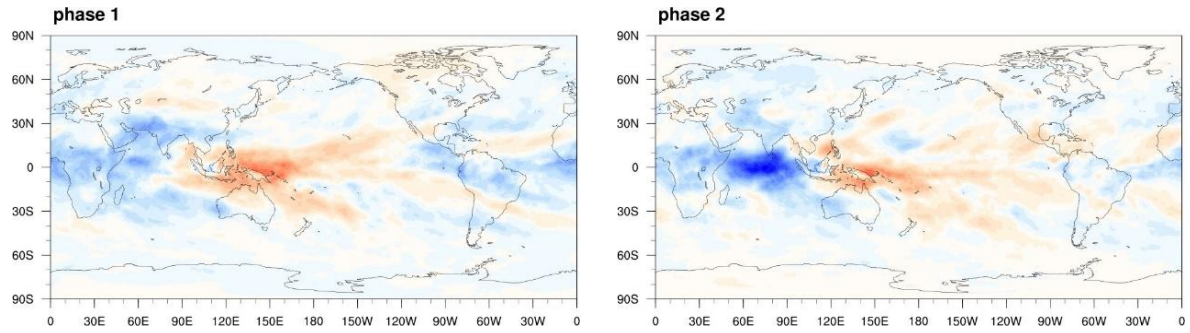

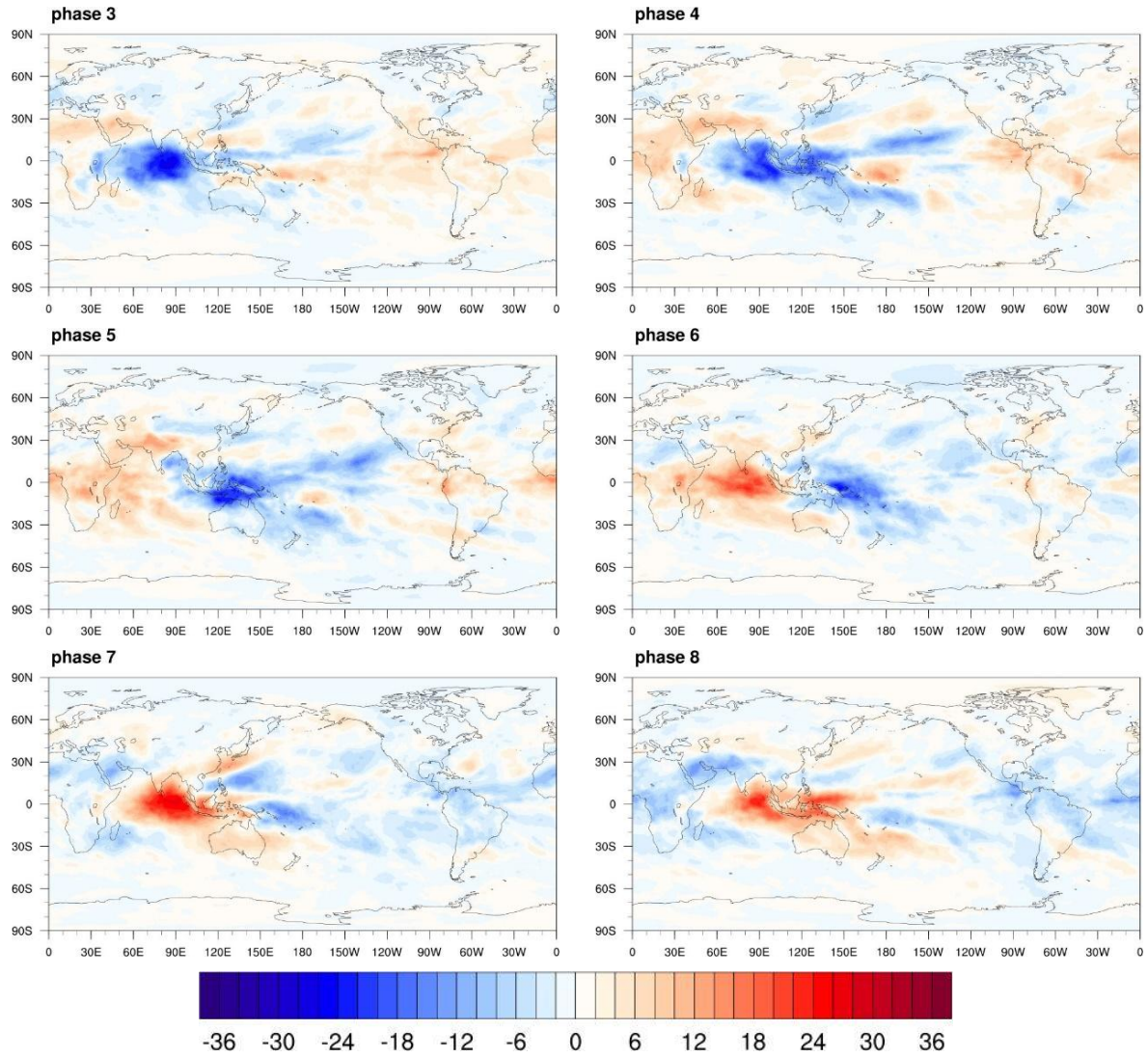

Figure 2: Anomalies of Spring composite OLRS in different MJO phases (units: W·m^-2).

Figure 2 displays an obvious east-west distribution of the winter OLR anomaly field. In Phase 1-2, there are abundant areas of negative OLR anomaly in the Western and Central Indian Ocean; At the same time, positive OLR anomalies extend farther eastward. In Phases III and IV, The centre of the negative anomaly moves to the maritime continental area, extending longitudinally; Some signals have even expanded across the mid-latitudes as well. During phases 5-6: As the enhancement of convection spreads westward across the South China Sea, a re-emerging suppressed-convection zone appears in the Eastern Hemisphere. According to Phase 7-8, there was a weakening of the negative centre and an eastward shift. Amplitude exceeds -30 dBm·m-2 in the strongest phase; Among these four seasons, the winter composite has the widest band of the tropical-to-extratropical transition.

The spring OLR composite retains the same phase progression, but the convective anomaly is weaker and less connected to the extratropical belt, as shown in Figure 3.

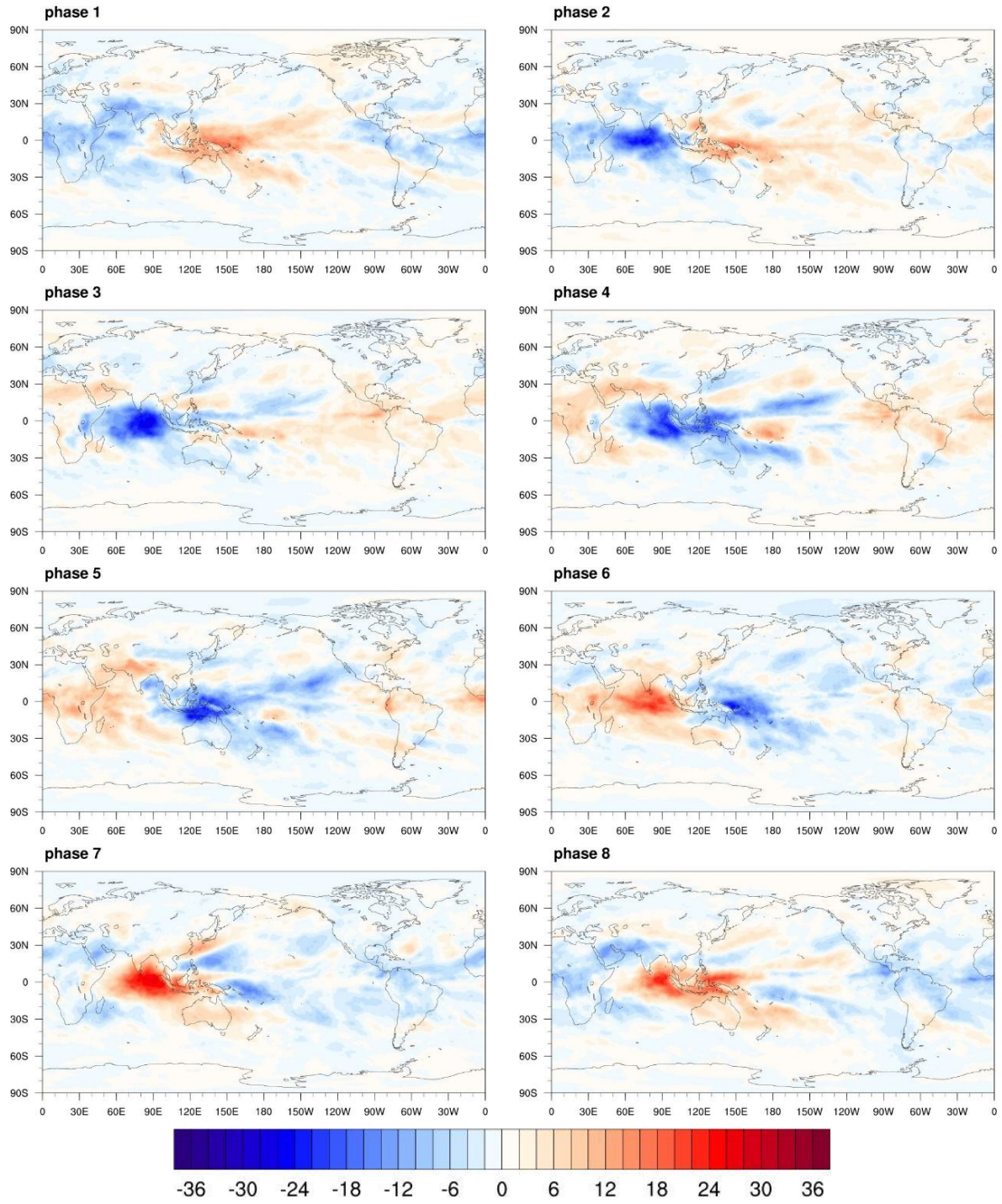

Figure 3: Spring composite OLR anomaly changes of MJO phase I~VIII (unit: W·m-2).

As shown in Figure 3, there is a relatively small deviation around −20 to −25 $W \cdot m^{-2}$ of the activity centre. The eastward advance from the Indian Ocean to the Maritime Continent and then into the western Pacific can still be identified; However, beyond the deep tropics, it becomes increasingly weaker compared with that of January. The seasonally weakened tropical heating anomaly may be less conducive to the generation of a robust Rossby wave system over Europe and East Asia. The spring composite therefore supports a weaker surface-temperature signal than the winter composite.

The summer composite is generally more pronounced than those of other times; see Figure 4.

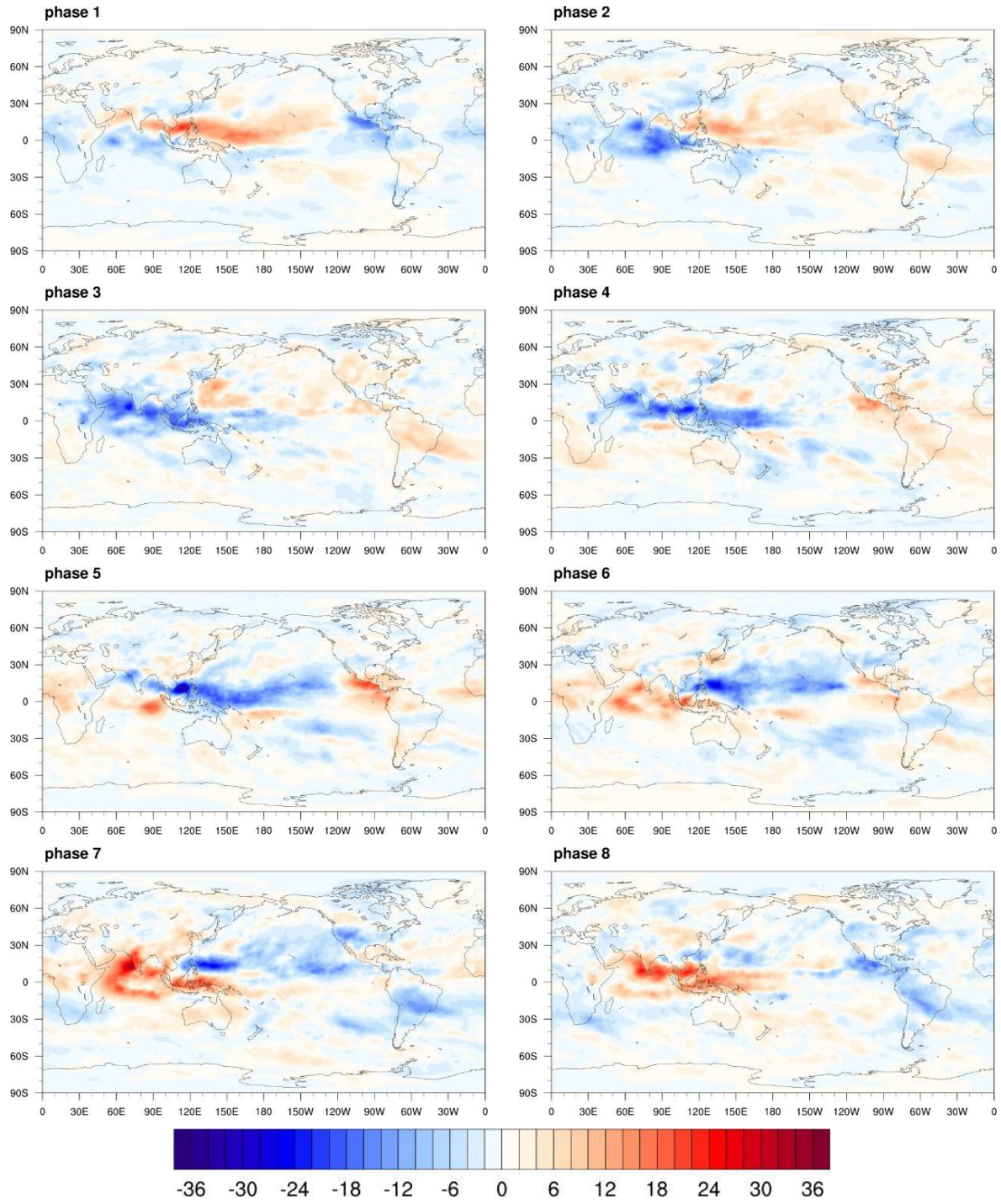

Figure 4: Summer composite OLR anomaly series by MJO phases, from 1 to 8.

Figure 4 indicates that summer MJO convection is narrow, weak and less spatially continuous. The centre of the OLR anomaly usually covers an area near the equator; at this time, it ranges from about -10 to -15 $W \cdot m^{-2}$. There are fewer coordinated features of the west-Pacific-centre-Pacific adjustment compared with that during summer; some phases have milder or even lacking convection. This kind of combination matches that dominated by the East Asian Summer Monsoon Background. In terms of temperature distribution in Shanxi Province, there are mainly two types: one type is generally cool with a lot of rain; The other is hot and dry.

The autumn OLRComposite presents an improvement in the convection strength of the MJO below its summertime low point; See Figure 5.

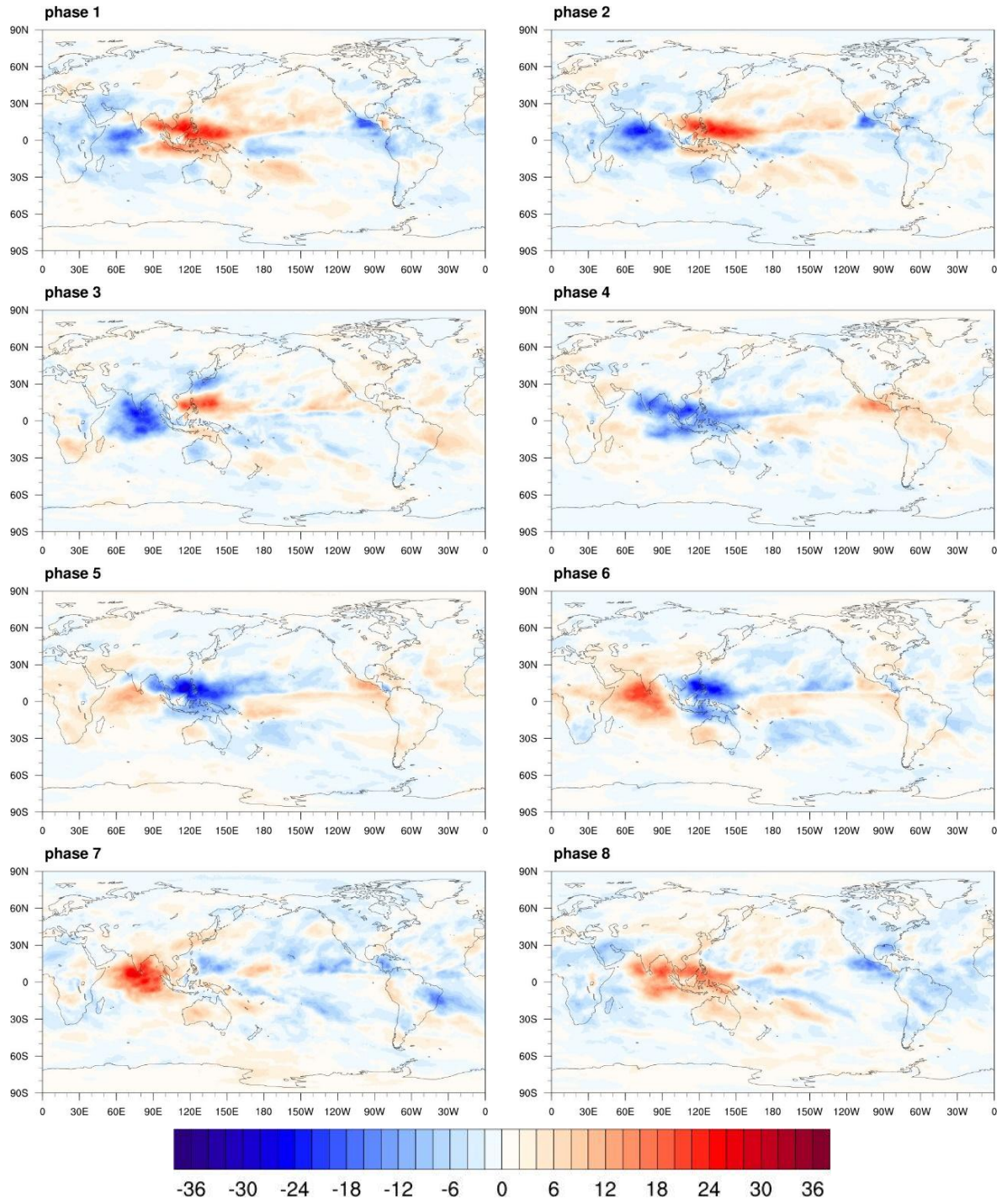

Figure 5: Autumn composite OLR anomalies of MJO phases 1-8 units (W·m^-2).

As shown in Figure 5, Autumn deviations are more prominent compared with Summer deviations and close to Winter phase ordering. A further negative OLR centre has moved from the Indian Ocean region towards the Maritime Continent and west of China, with maximum intensities between -25 to -30 ×10-6W·m^-2. Although there may be less meridional extension compared with winter, autumn fields show a stronger northern-hemispheric tropical-extratropical feature than those in spring. It provides a reference basis for identifying the greater Autumn temperature Response later on in Shanxi.

Combined with Figure 2-5 shows that the MJO convective source is seasonally asymmetrical. Winter has its most intense tropical forcing and the largest anomaly area;

Summer has relatively weak and discontinuous impact of such factors; Spring and Autumn function as transitional periods, being more similar to Winter's level of convection. This seasonality is the background condition of the temperature composite maps in Shanxi Province.

3.2 Phase-dependent surface-temperature response over Shanxi

Based on this, the following problem arises: Does the Shanxi area's surface temperature change in unison with MJO phases? Figures 6-9 show the season-specific T2M anomaly composites in Shanxi Province and its adjacent areas. Anomalies are mainly detected by their signs, amplitudes and phase concentrations; The winter period has the weakest response coherence among all seasons; Figure 6 shows that Shanxi is more coherent during this time than at other times.

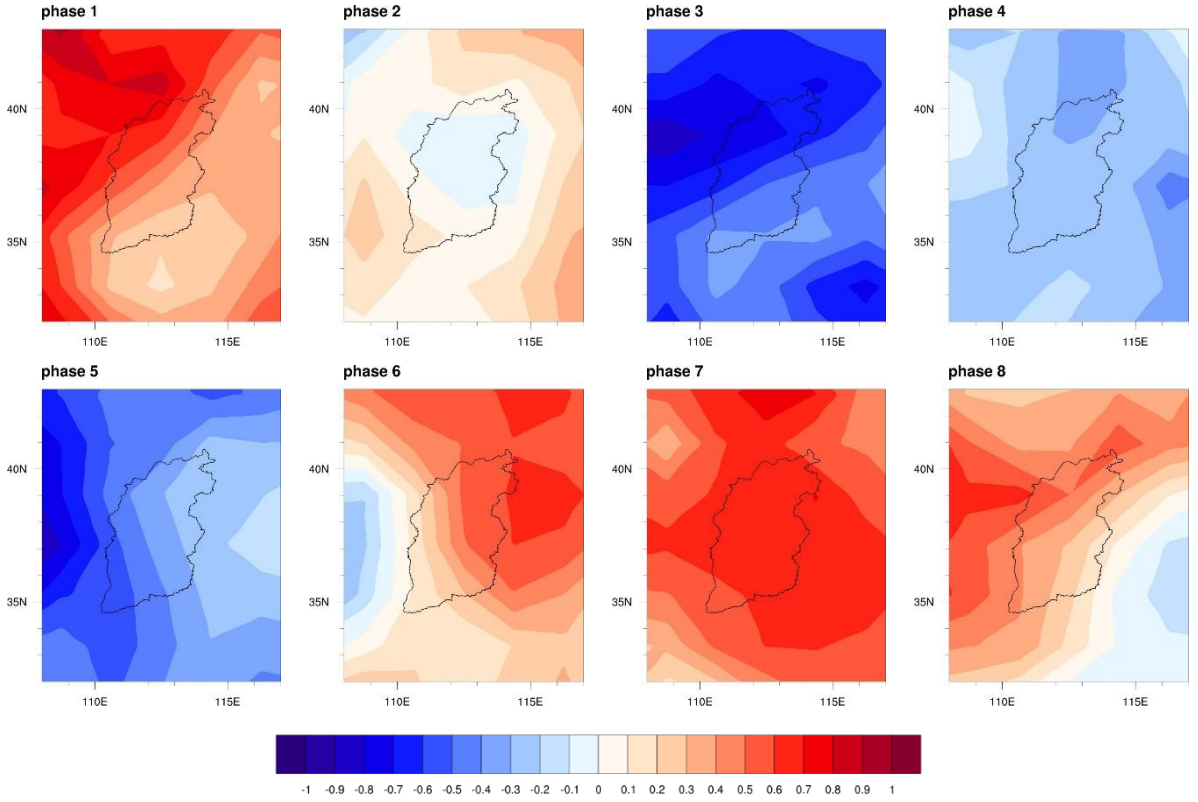

Figure 6: Winter composite T2M anomaly fields of Shanxi and nearby regions during MJO phases 1 to 8.

As shown in Figure 6, there is periodic alternating hot-cold anomaly states. Phase 1 has a relatively weak warm anomaly and there is an increasing strength of the anomaly moving from south to north. Phase 2 is no longer stable; there is a relatively small cooling signal at its core, and warmer or close-to-normal temperatures are observed nearby. Phase III has shown a greater degree of cold reaction, with the province-level anomaly around -0.8K. At phases 4-5 cold stimulation weakens; at phase six-eighth there will be an appropriate warming response. A warm peak appears around Phase 7 and has a magnitude close to 0.6K. The above structure shows that winter MJO forcing can influence the time and strength of cold air controlling Shanxi Province; In addition, when the tropical convection is located in the Indian Ocean-Western Pacific transitional region.

The spring Response is weaker, with different main periods from those in Winter; As shown in Figure 7.

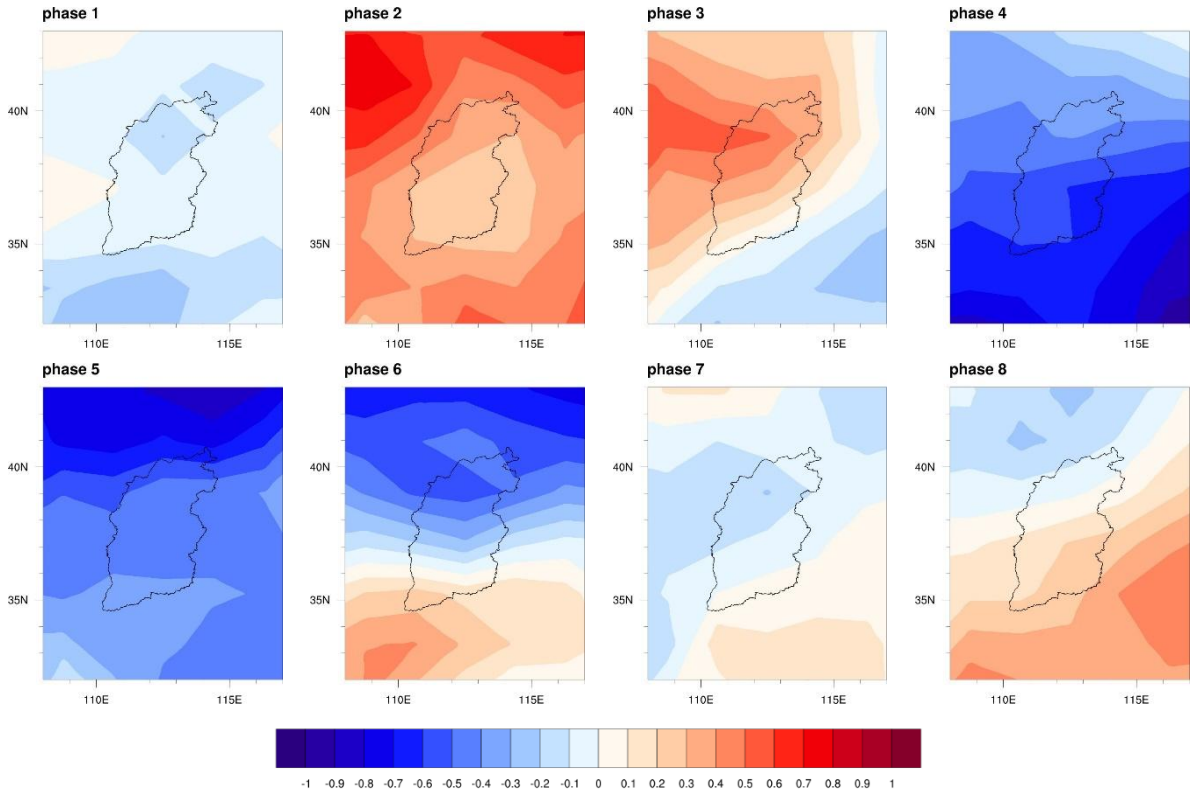

Figure 7: Spring composite T2M anomaly over Shanxi and nearby regions in MJO phase 1-8 (K).

Figure 7 shows that spring phase 2 is generally warm and phase 3 strengthens the warm signal. Phases 4-6 subsequently present as a cold anomaly, but its extent falls short of that in Phase 1. The sixth stage shows a weak warm anomaly in southwestern Shanxi; thus, the spatial pattern may be different from that of the winter sensitivity experiment. The other periods are very small or have scattered abnormalities. The spring feature indicates that although the MJO continues to influence this area through its impact on local temperature distribution; Under this background condition, the weakening of winter cold air passage and enhancement of early summer process are observed.

Summer shows the least coherent MJO-related surface-temperature response, as shown in Figure 8.

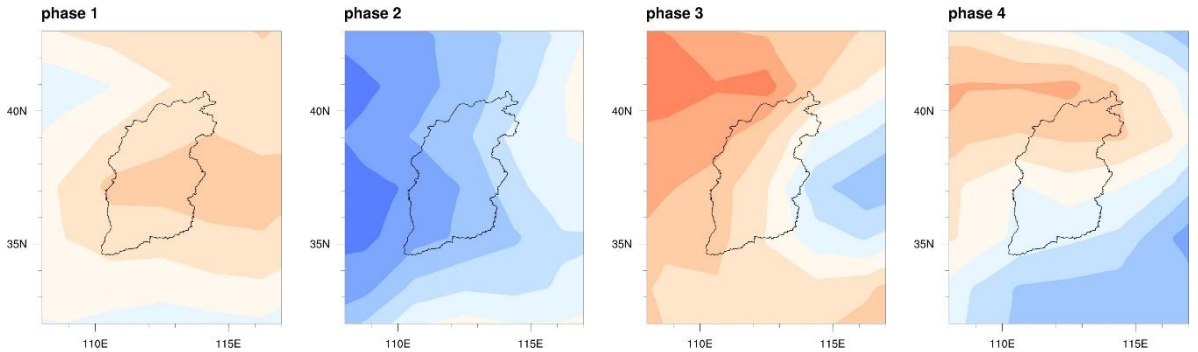

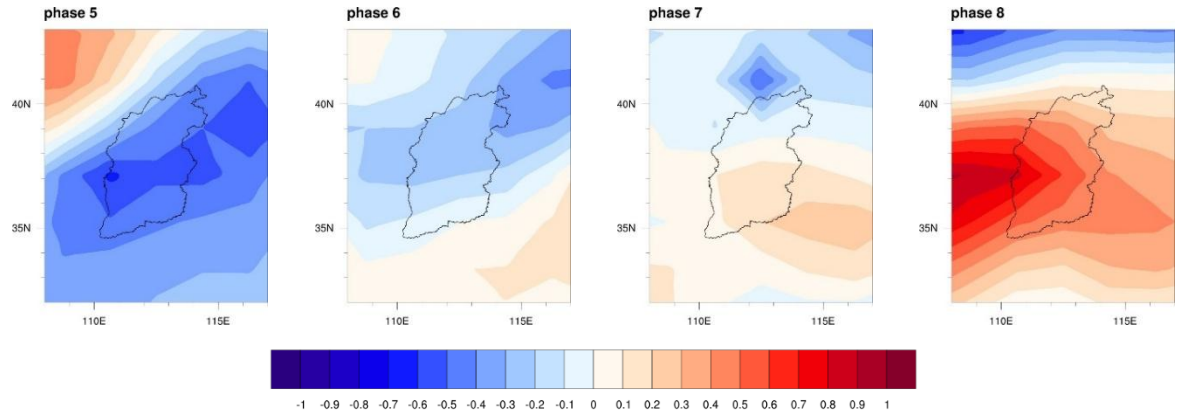

Figure 8: Summer composite T2M anomaly fields of Shanxi and adjacent regions across MJO phases 1 to 8.

As shown in Figure 8, most of the summer-phase composite materials in Shanxi are around 0K. Fluctuations are small during periods 5 and 8; however, there is no stable provincial-scale anomaly phenomenon across these periods. The above result is also consistent with the weak OLRSignal in Figure 4. Because of the lack of fast Modulation during summer, it cannot resist the development of intense Local convection triggered by external disturbances. There is no deficiency of an obvious MJO-related T2M signal; therefore, MJO may still have some impact on East Asian summer weather at the surface level; however, compared with other seasons, its phase-averaged response will weaken significantly because of the dominant effect of the background circulation patterns.

Figure 9 shows that the autumn response is reinforced again and has a significant positive anomaly at the end of the MJO cycle;

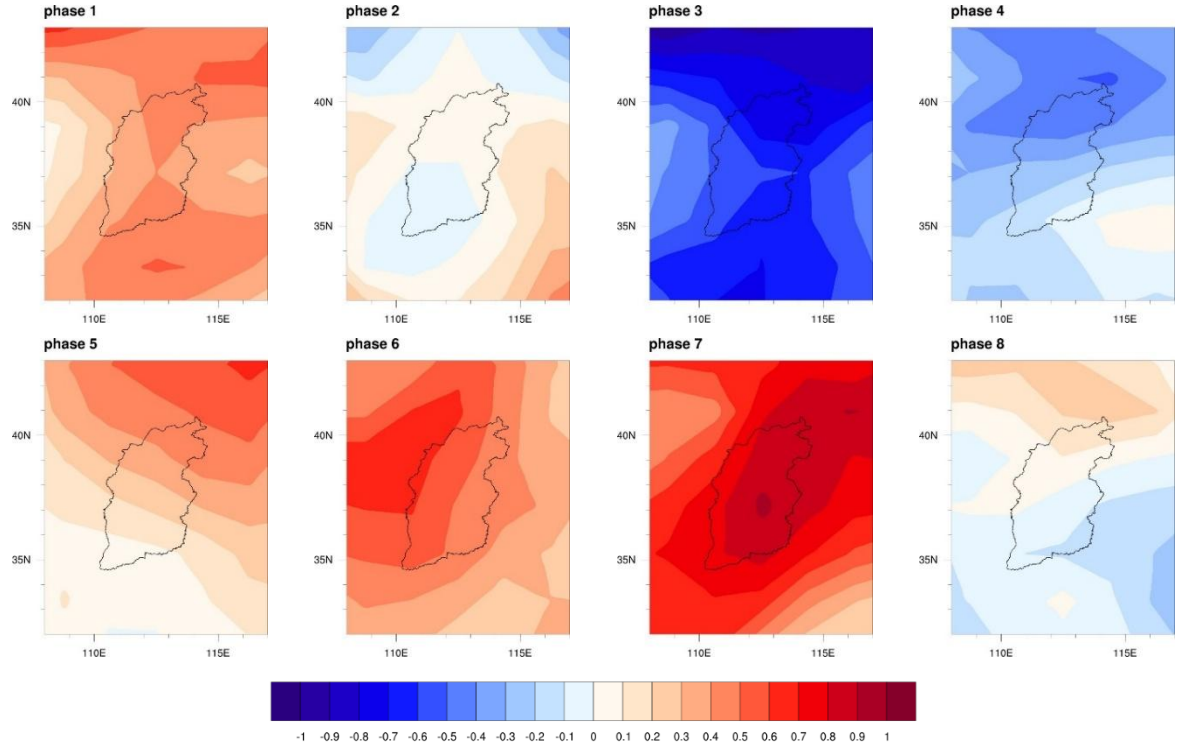

Figure 9: Composite T2M anomaly fields over Shanxi and its adjacent areas for MJO phase 1-8.

Figure 9 shows that phase 1 is warm over much of Shanxi, phase 2 approaches near-normal conditions, and phase 3 becomes the main cold phase with an anomaly near -0.7 K. Phase 4-5 is a cool-warm transformation period; In phases 5-7, there will be an increasing warmth anomaly. In phase 7, the central part of Shanxi has reached a warm anomaly more than one standard deviation away from its winter warmest state. Back to a normal phase eight. The autumn result is clear; there is no warmth in a subdued way, nor is there snowfall. The circulation background at this time is more favourable for converting west-pacific MJO forcing to a warm anomaly over Shanxi Province; that is, with weakened cold-air intrusion and enhanced warming advection.

Obtained compact summarizations of the phase-season response based on the primary abnormal data shown in Figure 6-9, respectively. As shown in Figure 10, this value is arranged to form an eight-Phase, four-School pattern Matrix structure.

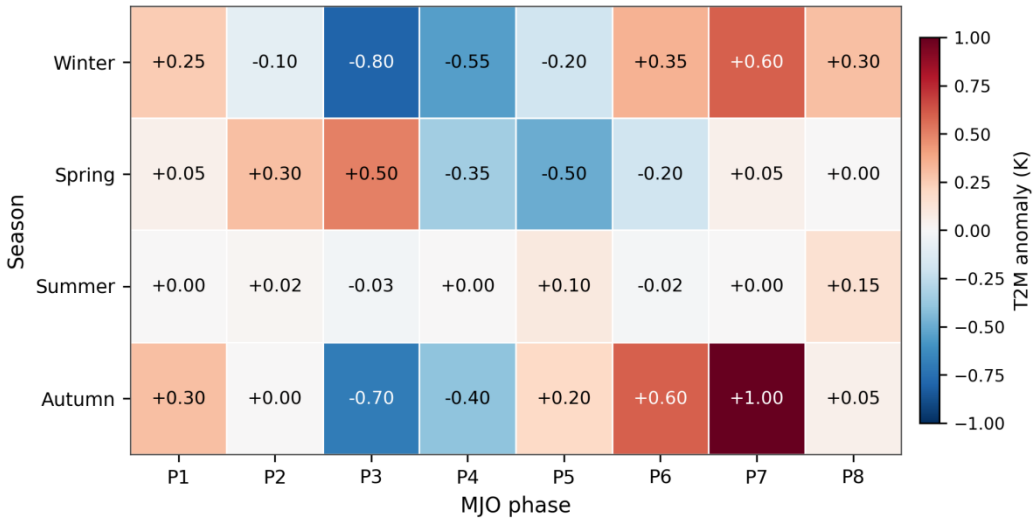

Figure 10: Synthesis Matrix of Phase-Seasonal Synthesis Anomalies in T2M for Shanxi Derivations Based on Seasonal Composites.

Figure 10 shows the following. First of all, the winter and autumn with the greatest absolute values at present are about -0.80K and +1.00K, respectively, as shown in Table 5-6. Secondly, the remaining time of summer across most seasons is very near 0°C and cannot serve as an excellent temperature indicator for Shanxi. Thirdly, the warm-cold alternations of different times do not occur simultaneously. Winter cold anomaly areas cluster around phase 3, and autumn exhibits this pattern; However, the warm area at this time point is relatively significant. The seasonal migration of this phenomenon is necessary to consider during interpretation because it will not apply continuously within all seasons.

In addition, it shows that a single year-over-year phase-Response rule cannot work. Phase three has been cold in the Winter and Autumn, but it's Hotter in Spring. During the weak Warm signal phase in Phase 7 is not directly related to Temperatures from Summer. The season-dependent dependency indicates that the MJO need to be entered into an extended-range temperature service via a seasonal look-up table instead of a single-phase identifier. The sign and strength of the reaction need to be evaluated together with the background season.

Table 2: Seasonal summary of MJO phase effects on Shanxi surface temperature.

Season	Dominant cold phase(s)	Dominant warm phase(s)	Approximate anomaly range	Interpretive meaning
Winter	Phase 3-4	Phase 6-8	-0.8 to +0.6 K	Strongest and most coherent MJO-temperature coupling
Spring	Phase 4-6	Phase 2-3	-0.5 to +0.5 K	Weaker response under transition-season circulation
Summer	No stable phase	No stable phase	Near 0 K	MJO signal masked by monsoon and local thermal processes
Autumn	Phase 3-4	Phase 5-7	-0.7 to +1.0 K	Recovered teleconnection with strong late-phase warm response

Table 2, as in Figures 10-8 to 10-31: provides similar explanations and physical meanings of responses corresponding to different seasons; Winter and autumn are the primary seasons for MJO phases to function as a sub-seasonal prediction tool. Spring needs to be more cautious due to its relatively larger anomaly amplitude and less even spatial response. Summer provides minimal contributions to phase-based temperature predictions in Shanxi under this combined method.

It can only be used for reference in application; it will not constitute an actual forecasting equation after being referred to. When there is an active MJO event in winter Phase 3 or autumn Phase 3, the prediction of meteorological conditions will check whether a negative-height-anomaly-field forms in northern China or a deeper-East-Asian-trough appears at the same time. When the event enters winter phase 7 or autumn phase 7, in turn, a similar operation process for positive-height anomaly, weakened-cold-air-pathway and warm-advective signal is adopted. Therefore, The MJO stage can provide a time-lagged background; While the circulation pattern indicates whether it is sufficient for heating Shanxi temperatures.

3.3 Teleconnection mechanism and implications for extended-range temperature prediction

The Surface-Temperature Composites need to be circled, and Shanxi is away from the tropic convection region. By remote route (due to an abnormal increase in tropical heat caused by MJO anomaly disturbance on global planetary waves), the form of eastern monsoon area will change subsequently, which leads to differences in cold-core and warm front advection types from northeastern China. Tropical OLR anomaly can be connected with Shanxi's air temperature through a bridge of the 500-hPa height field.

This mechanism has no need for the direct tropical-to-Shanxi thermal connection. Tropical variability first alters the distribution of diabatic Heating; Then in response to this change, the atmosphere reorganises Wave Activity and Height Anomalies along preferred mid-Latitudinal Pathways. When the wave response project onto an Eurasia-PacifiC Pattern, a resultant-height anomaly may cause the trajectory of the East-Asia Trough to change, modify meridional flow and reduce cold-air penetration events. Then the Shanxi temperature is affected by advection, subsidence and cloud-radiation under such a circulating environment.

In winter, Phases 3-4 are primarily cold in Shanxi Province. When there is active convection over the Indian Ocean or the Maritime Continent area, this heating anomaly may promote an EWP (Eurasian Wave Pattern) where trough formation in eastern China is more pronounced. A negative five hundred pressure-highness anomaly in Eurasia has intensified the Eastern Asia

trough and maintained a northward movement of cold air. In this situation, Shanxi Province will be downstream of the cold-air-originating area and remain vulnerable to persistent low-temperature events. A cold anomaly of about -0.8K during the Winter Phase III, which means it may be undertroughed or have strong frequency of cold air intrusions.

The winter warming periods are generally in Phases 6-8. When the primary MJO convection centre advances towards the western Pacific, it will cause a weakening of trough control in northern China and support the emergence of positive five-hundred-pressure-centre-height anomaly patterns near or downstream of Shanxi. A positive height anomaly decreases the southward propagation of cold air masses and favours warm advection from the south-west or west. Therefore, a weak surface response is obtained; there is also coherence in this phenomenon; The temperature anomaly near 1.5 °C appears around phase-7. Aisymmetry in the cold- and warm-amplitude Distribution is derived theoretically by analyzing the different intensity-changing mechanisms resulting from cold air outbreak or warmth advection fronts in continental settings, respectively.

Spring still has the path of teleconnection, but the strengthening power is reduced. The mid-latitudinal westerly jet decreases relative to that in winter; parts of cold-source areas have weakened thermodynamic contrasts, and the eastward advance of the seasonally varying flow pattern begins. There are still MJO-related height anomalies at times, but they are relatively weaker and lack clear spatial structure over northern China. Because of this, the phase II-III produces weak warm anomaly, and phase IV - VI produces weak cold abnormality; Many spring periods are still near-normal levels. Spring forecasts based only on MJO phase should therefore be combined with background circulation indicators such as trough position, blocking activity and the strength of meridional flow.

The summer season has a lessened impact of the teleconnection pathway on Shanxi temperatures. OLR composite: Weak tropical convective activity; Monsoon regime in the northern hemisphere with a dominance of subtropical-high variability and local land-atmosphere interaction effects. Processes that shorten the reorganisation time of the temperature field compared to the MJO composite window. Whether or not there is a weak MJO-related signal aloft, it may be unable to remain as an independent provincial-level T2M anomaly. The near-zero summer response shown in Figures 8 and 10 should thus not be regarded as an indication of the MJO's lack of activity globally but rather that there may be issues with the application of phase-based temperature diagnosis.

Autumn is very different from summer clearly. When the monsoon is weakening and the westerlies become stronger, then the mid-latitude path will reappear again. From Phases 3-4, there are relatively weak cold anomalies; From Phases 5-7, there is a more pronounced warming. Approximately 1.0K increase in the phase-7 anomaly suggests that there is an outstanding connection between autumn warm events in Shanxi and a delayed-stage MJO circulation system. Compared with winter, the autumn warming anomaly may be enhanced due to a background of reduced early cold air outbreaks but allow western Pacific wave energy to reach East Asia [10-19].

Extended-range prediction is not recommended for the use of seasonal constraints on MJO information. In winter, Phases 3-4 may be regarded as cold anomaly signals, while Phases 6-8 could indicate warmth anomalies. The tenth of a month has the risk of cold phases or warm spells. The Spring phase information may serve as another signal, and its weak amplitude should also undergo multiple confirmations. Only summer-phase characteristics have little to do with changes in temperature; They are weak across different areas and spread out.

In addition, there are also some limitations in the current empirical Design. The composites show phase-specific mean response over the next four decades; however, there is no distinction of fast-slow MJO propagation speed and amplitude class boundaries nor interaction effects

involving ENSO and Arctic-MIDLFC mode systems. Terrain effects within Shanxi Province are reflected indirectly through the grid-averaged T2M fields [20-25]. Future work should combine reanalysis data with station observations, divide MJO events by propagation speed and amplitude, and test whether the phase-response rules improve real extended-range forecasts of cold waves, warm spells and frost-risk periods in Shanxi.

Uncertainty also exists in transforming a large-scale circulation into local Land temperature; High-altitude terrain, intra-montane Basin and Valley System in Shanxi province cause an inversely proportional relationship between mountain boundary surfaces and temperature changes. Composite maps display a generalised signal; station-by-station verification should be conducted to see if the same-phase-response effect holds universally across northern plateau stations, central Basin Stations and southern Valley Stations. For use of this method in local warnings, it needs to pass through this stage even if we are talking about nationwide climate analysis only.

4 Conclusion

Based on the 1985-2025 period of daily RMM indices, OLR, T2M and 500-hPa geopotential height data for studying the impact of atmospheric internal fluctuations on surface temperatures in Shanxi Province. Organised by seasons and the MJO stage to evaluate separately in each case the origin of tropical convection, the local change in temperature and the global circulation system triggered.

(1) According to OLR composite data showing an identical Eastern-shift phenomenon seasonally; however, the severity differs across regions. Winter has the most significant and extensive OLR anomaly patterns; convective activity covers deeper latitudes. Summer exhibits weaker or narrower abnormal areas. Spring and autumn are transition seasons, with autumn closer to winter in the strength and continuity of the convective signal.

(2) There is obvious seasonal difference in surface temperatures over Shanxi related to MJO phases. In winter, there is the most pronounced coherently responsive phenomenon; The cold anomaly of phase-III reaches up to -0.8K, and the warm anomaly of phase-VII exceeds +0.6K. Spring has an attenuated Phase Response. Summer shows no stable province-wide anomaly. Autumn is getting stronger; the third-phase cold anomaly is around -0.7K, and the seventh-phase warm anomaly has reached close to +1.0K locally.

(3) The physical Pathway is largely isolated. MJO-triggered tropical convection can change the extratropical circulation via Rossby wave propagation and associated Eurasian or Western-Pacific teleconnection patterns. Negative-500-hPa-height anomaly areas in the north of China favour trough formation and cold air entrainment; Positive-500-hPa-height anomaly areas reduce cold-air activity and enhance warm-air advection. Accordingly, it is possible to conclude that the sub-seasonal change model (MCM) holds some meaning for forecasting the temperature changes of winter in Shanxi Province; Nevertheless, due to problems remaining unsolved yet-to-be-solved at present, it cannot be applied currently.

Funding

This work was supported by Shanxi Provincial Meteorological Bureau.

About the Author

JinXia Wang was born in Shuozhou, Shanxi, China, in 1999. She obtained a bachelor's degree

from Nanjing University of Information Science and Technology in China.She is currently working at the Yangquan Meteorological Bureau. Her main research direction is climate change.

Yan Wang was born in Yangquan, Shanxi, China, in 1992. She obtained a master's degree from Chengdu University of Information Technology in China. She is currently working at the Yangquan Meteorological Bureau. Her main research direction is cweather forecasting.

ZiYu Yan was born in Yangquan, Shanxi, China, in 1996. He obtained a bachelor's degree from Wuchang University of Technology in China. He is currently working at the Yangquan Meteorological Bureau. His main research direction is communication engineering.

References

[1] Lin, H. (2022). The Madden-Julian Oscillation. Atmosphere-Ocean, 60(3–4), 338–359.

[2] Kikuchi, K. (2021). The Boreal Summer Intraseasonal Oscillation (BSISO): A review. Journal of the Meteorological Society of Japan, 99(4), 933–972.

[3] Zhang, C. (2013). Madden-Julian Oscillation: Bridging weather and climate. Bulletin of the American Meteorological Society, 94(12), 1849–1870.

[4] Wheeler, M. C., & Hendon, H. H. (2004). An all-season real-time multivariate MJO index: Development of an index for monitoring and prediction. Monthly Weather Review, 132(8), 1917–1932.

[5] Lee, J. Y., Wang, B., Wheeler, M. C., et al. (2013). Real-time multivariate indices for the Boreal Summer Intraseasonal Oscillation over the Asian summer monsoon region. Climate Dynamics, 40, 493–509.

[6] Jeong, J. H., Ho, C. H., Kim, B. M., et al. (2005). Influence of the Madden-Julian Oscillation on wintertime surface air temperature and cold surges in East Asia. Journal of Geophysical Research: Atmospheres, 110, D11104.

[7] Kim, S., Kug, J. S., & Seo, K. H. (2020). Impacts of MJO on the intraseasonal temperature variation in East Asia. Journal of Climate, 33(20), 8903–8916.

[8] Song, L., Wu, R., Jiao, Y., et al. (2019). Combined effects of the MJO and the Arctic Oscillation on the intraseasonal eastern China winter temperature variations. Journal of Climate, 32(8), 2275–2291.

[9] Chang, C. H., Johnson, N. C., & Yoo, C. (2021). Evaluation of subseasonal impacts of the MJO/BSISO in the East Asian extended summer. Climate Dynamics, 56, 3553–3568.

[10] Hsu, P. C., Lee, J. Y., Ha, K. J., et al. (2017). Influences of Boreal Summer Intraseasonal Oscillation on heat waves in monsoon Asia. Journal of Climate, 30(18), 7191–7211.

[11] Diao, Y. F., Li, T., & Hsu, P. C. (2018). Influence of the Boreal Summer Intraseasonal Oscillation on extreme hot and cool events in China. Journal of Meteorological Research, 32(4), 534–547.

[12] Tang, Y., Ren, H. L., Zhang, P., et al. (2022). Intraseasonal oscillation of summer extreme high temperature in Northeast China and its associated atmospheric circulation.

Atmosphere, 13(3), 387.

[13] Hao, L., He, J., Wang, H., et al. (2023). Influence of Boreal Summer Intraseasonal Oscillation on summer precipitation in North China. International Journal of Climatology, 43(12), 5618–5634.

[14] Hersbach, H., Bell, B., Berrisford, P., et al. (2020). The ERA5 global reanalysis. Quarterly Journal of the Royal Meteorological Society, 146(730), 1999–2049.

[15] Muñoz-Sabater, J., Dutra, E., Agustí-Panareda, A., et al. (2021). ERA5-Land: A state-of-the-art global reanalysis dataset for land applications. Earth System Science Data, 13(9), 4349–4383.

[16] Wan, Z., Hook, S., & Hulley, G. (2021). MODIS/Terra Land Surface Temperature/Emissivity Daily L3 Global 1 km SIN Grid V061. NASA LP DAAC.

[17] Wang, W., Duan, S. B., Min, X., Guan, Y., Wei, R., & Li, Z. (2025). Integrating Split-Window and Temperature-Emissivity Separation Algorithms for Hourly Land Surface Temperature Retrieval From GOES-16 ABI Data. IEEE Transactions on Geoscience and Remote Sensing, 63, 1-13.

[18] Wan, Z. (2014). New refinements and validation of the collection-6 MODIS land-surface temperature/emissivity product. Remote Sensing of Environment, 140, 36–45.

[19] Duan, S. B., Li, Z. L., Li, H., et al. (2019). Validation of Collection 6 MODIS land surface temperature product using in situ measurements. Remote Sensing of Environment, 225, 16–29.

[20] Farr, T. G., Rosen, P. A., Caro, E., et al. (2007). The Shuttle Radar Topography Mission. Reviews of Geophysics, 45, RG2004.

[21] Liebmann, B., & Smith, C. A. (1996). Description of a complete (interpolated) outgoing longwave radiation dataset. Bulletin of the American Meteorological Society, 77(6), 1275–1277.

[22] Duchon, C. E. (1979). Lanczos filtering in one and two dimensions. Journal of Applied Meteorology, 18(8), 1016–1022.

[23] Ghil, M., Allen, M. R., Dettinger, M. D., et al. (2002). Advanced spectral methods for climatic time series. Reviews of Geophysics, 40(1), 3-1–3-41.

[24] Benjamini, Y., & Hochberg, Y. (1995). Controlling the false discovery rate: A practical and powerful approach to multiple testing. Journal of the Royal Statistical Society: Series B, 57(1), 289–300.

[25] Wilks, D. S. (2006). On field significance and the false discovery rate. Journal of Applied Meteorology and Climatology, 45(9), 1181–1189.